EFFECTS OF PWHT TEMPERATURE ON MECHANICAL PROPERTIES OF HIGH-Cr FERRITIC HEAT-RESISTANT STEEL WELD METALS

L. Chen and K. Yamashita

ABSTRACT

Welded joints of ASME Gr. 91 steel are subject to post-weld heat treatment (PWHT) to obtain sufficient mechanical properties. However, when the PWHT temperature is higher than the lower critical transformation temperature (A_{C1}) of both the base metal and the weld metal, the mechanical properties of the weld may be degraded. To avoid this, it is important to know the A_{C1} of the weld. The authors have investigated several methods of measuring the A_{C1} of Gr. 91 steel weld metals to select the most credible method and examined the effects of the PWHT temperature on the mechanical properties of the weld metal. In addition, the proper PWHT temperature was discussed in consideration of the measurements of A_{C1}, test results of creep-rupture performance, and observation results of precipitates. In the case of a low Mn+Ni weld metal, the upper PWHT temperature limit should be lower than A_{C1}. On the other hand, in the case of the high Mn+Ni weld metal, remarkable negative effects on the mechanical properties of the weld metal were not found, even though the PWHT temperature exceeds A_{C1} by about 30 °C.

IIW-Thesaurus keywords: Critical values; Mechanical properties; Post weld heat treatment; Temperature; Transformation; Weld metal.

1 Introduction

From the view point of oxidation resistance, linear expansion coefficient and high-temperature strength, ASME Gr. 91 steel is used as a major material for large-diameter heavy-wall pipes such as the main steam pipe for thermal-power boilers, which are used in high-temperature high-pressure environments. Gr.91 steel, commonly referred to as Modified 9Cr-1Mo or P91, was originally developed from conventional 9Cr-1Mo grades by the Oak Ridge National Laboratory for application in fast breeder reactors. Modifications include additions of vanadium, niobium, nitrogen and lower carbon content. When produced and heat treated to form the proper microstructure, it provides excellent elevated-temperature properties [1-4]. In order to secure the mechanical properties of the Gr. 91 steel weld metals, such as creep-rupture performance and impact toughness, the welded joints are subject to PWHT under the suitable conditions to form the fine temper martensite microstructure with a large number of fine carbonitride precipitates. However, if the PWHT temperature is excessively low, the prescribed impact toughness cannot be obtained; conversely, if it is excessively high, the creep-rupture performance becomes degraded [5-7]. The PWHT temperature is set to be lower than A_{C1} of the weld metal in general; nevertheless, it is important for selecting the most appropriate PWHT conditions to understand what can occur in the weld metal if the actual PWHT is conducted within a temperature range that noticeably exceeds A_{C1}.

For determining an appropriate PWHT temperature, it is significant to know the precise A_{C1} of the weld metal in advance. Several methods for measuring A_{C1} have been reported, such as that detecting expansion and contraction induced by the phase transformation [8-10], Differential Thermal Analysis (DTA) [11], Single Thermocouple Differential Thermal Analysis (STC DTA) [12], in-situ diffraction measurement [9], thermodynamic modelling [10], ultrasonic velocity measurements [13]. In addition, the predominant method for measuring A_{C1} is standardized to ASTM 1033-04 [14] and SEP 1681 [15]. However, the measurements of A_{C1} may largely vary, depending on the measuring method and conditions [16]. If a PWHT temperature is decided in reference to an actual measurement different from the true A_{C1}, it may not be appropriate. Furthermore, it is well-known that A_{C1} significantly varies depending on the manganese (Mn) and nickel (Ni) contents in the weld metal [17]; however, there has been almost no research report on how a PWHT temperature above A_{C1} affects the microstructure and mechanical properties of the weld metal in relation to different amounts of Mn and Ni in the weld metal. In the present study, the authors have tested several methods for measuring the A_{C1} of two kinds of Gr. 91 steel weld metals containing

Doc. IIW-2177, recommended for publication by Commission IX "Behaviour of Metals Subjected to Welding."

different amounts of Mn and Ni to select the most credible measuring method, and have suggested how to determine the most suitable PWHT temperature associated with the Mn and Ni contents of the weld metal, taking into account the effect of PWHT temperature on the microstructure and mechanical properties of the weld metal.

2 Considerations on several A_{C1} measuring methods and measurements

2.1 A_{C1} measuring methods

A_{C1} is defined as the temperature at which the austenitic phase (γ-phase) begins to generate during the heating process. The methods for measuring A_{C1} include one that uses the expansion and contraction induced by the phase transformation of the test specimen and another (DTA: Differential Thermal Analysis) that uses the exothermic and endothermic reactions. In measuring A_{C1} by these methods, the measuring accuracy of expansion, contraction and temperature governs the correctness of measurements; also, such measuring conditions as the heating rate of the test specimen and the measuring atmosphere are the key factors.

2.2 Test materials

Weld metals (A) and (B) shown as the test materials in Table 1 are typical of those made with the shielded metal arc welding electrodes for Gr. 91 steel. The two test materials differ specifically in the amount of austenite formers of Mn and Ni. These materials were prepared so that they differ in the Mn+Ni content because this content of the weld metal influences A_{C1} much more than other elements. Since there are only few reliable reference data of A_{C1} of such a high-Cr material, the A_{C1} of a standard test material made of carbon steel with 0.19 % C was also measured simultaneously in order to assess the reliability of the measurements of the high-Cr materials in the use of different measuring methods and conditions.

2.3 A_{C1} measuring methods and measurements

A_{C1} was measured on each test material by using the three different methods shown in Table 2. Method (1) measures the dimensional change in length of the specimen in a nitrogen atmosphere by using a measuring apparatus utilizing induction heaters and a linear variable differential transformer (LVDT). Method (2) measures the dimensional change in diameter of the specimen in a high vacuum by using a measuring apparatus utilizing induction heaters and a high-accuracy LED. Method (3) measures the differential temperature between measured specimen and standard specimen in an Ar atmosphere by using a DTA apparatus. For the three methods, the heating rate of the specimens was set to 10 °C/s up to 600 °C, and then, the specimens were heated at a lower rate of 5 °C/min in the range 600 °C-1 050 °C where reverse transformation would occur. Since austenite formation is a typical nucleation and growth phenomenon, the transformation temperature is expected to be sensitive to the heating rate [16], which should be set as low as possible to obtain a truer A_{C1} value. Furthermore, since the PWHT heating rate is less than 5 °C/min, the heating rate for measuring A_{C1} was set to 5 °C/min or less. The measuring results of A_{C1} are shown in Table 2 together with the measuring methods and conditions. Clearly, the measurements in the table are different depending on the measuring method. In consideration of the A_{C1} transformation temperature of carbon steel with 0.19 % C, approximately 727 °C in a Fe-C equilibrium diagram, the measurements by Method (2) that used a high-accuracy LED in the high-vacuum atmosphere and the DTA Method (3) can presumably be closer to the true value when compared to the mechanical type Method (1) with an LVDT in the nitrogen atmosphere. On the other hand, with the DTA Method (3), A_{C1} could not clearly be determined at times. From these testing results, the measurements by Method (2) was judged as the most reliable among the three methods. The reason why the A_{C1} measurements obtained by the mechanical type Method (1) with an LVDT deviated from those measured by the selected Method (2) has not been clarified; however, the oxide film generated on the test specimen surface during measurement was probably a cause.

2.4 Considerations on A_{C1} measurement conditions

Measurements of A_{C1} may possibly be scattered by being affected by the measuring conditions. To clarify this, the individual effects of specimen size, heating rate, and measuring atmosphere were investigated by using the equipment for measuring Method (2). In this study, the standard measurement was made by using a 8 mm Ø × 66 mm L specimen, a heating rate of 2 °C/min, and a high-vacuum atmosphere of 10^{-3} Pa.

Measurements of A_{C1} are shown as a function of specimen size in Figure 1 and as a function of heating rate in

Table 1 – Chemical composition of test materials [mass %]

Test materials	C	Si	Mn	Ni	Cr	Mo	V	Nb	N	Mn+Ni
Weld metal (A)	0.07	0.35	1.57	0.92	8.86	1.02	0.24	0.025	0.029	2.49
Weld metal (B)	0.11	0.23	0.85	0.53	9.01	1.01	0.25	0.034	0.028	1.38
Carbon steel with 0.19 %C	0.19	0.10	0.03	-	-	-	-	-	-	0.03

Table 2 – Measuring methods and results of A_{C1}

	No.	(1)	(2)	(3)
Measuring methods	Measured quantity	Dimensional change in length	Dimensional change in diameter	Differential temperature (DTA)
	Measuring device	LVDT (mechanical)	LED beam (non-contact)	Thermocouples
Measuring conditons	Specimen size	3 mm Ø × 10 mm L	8 mm Ø × 66 mm L	3 mm Ø × 2.5 mm L
	Heating rate	10 °C/s (RT-600 °C) - 5 °C/min (600-1 050 °C)		
	Atmosphere	N_2 after vacuumizing [b]	high vacuum [b]	flowing Ar after vacuumizing [b]
A_{c1} [a] Measuring results (°C)	Weld metal (A) (Mn + Ni = 2.49 %)	696	733	Could not be determined
	Weld metal (B) (Mn + Ni = 1.38 %)	758	785	795
	Carbon steel with 0.19 % C	699	732	731
Remarks		Oxide film generated on specimen surface during measurement	No oxide film generated on specimen surface during measurement	

[a] A_{c1} was determined as the point that deviated from the line relationship of dilatation or ΔT vs. temperature curve.
[b] Vacuum degree:10 Pa [Measuring Method (1)], 10^{-3}Pa [Measuring Method (2)], 10^{2}Pa [Measuring Method (3)]

Figure 2. The dilatation-temperature curves measured in the high (10^{-3} Pa) and low vacuum (10^{2} Pa) atmospheres are shown in Figure 3. Views of the specimens after measurement are shown in Figure 4.

The effects of the measurement conditions on A_{C1} are summarized in the following.

1. No effect of specimen size is observed (Figure 1).
2. A_{C1} becomes higher as the heating rate increases (Figure 2). Since the reverse transformation from ferrite to austenite together with the phenomenon of nucleation and its growth take time to occur, it is expected that the heating rate should be set as low as possible to obtain a truer A_{C1} value.
3. A_{C1} is likely to scatter depending on the measurement atmosphere, being affected by the oxide film formed on the specimen surface during measurement; this is owing to deteriorated accuracy in the measurement of dilatation (Figures 3 and 4).

3 Effects of PWHT temperature on mechanical properties

It is important to use an appropriate PWHT temperature in order to fabricate welded joints with sufficient impact toughness and creep-rupture performance in the use of

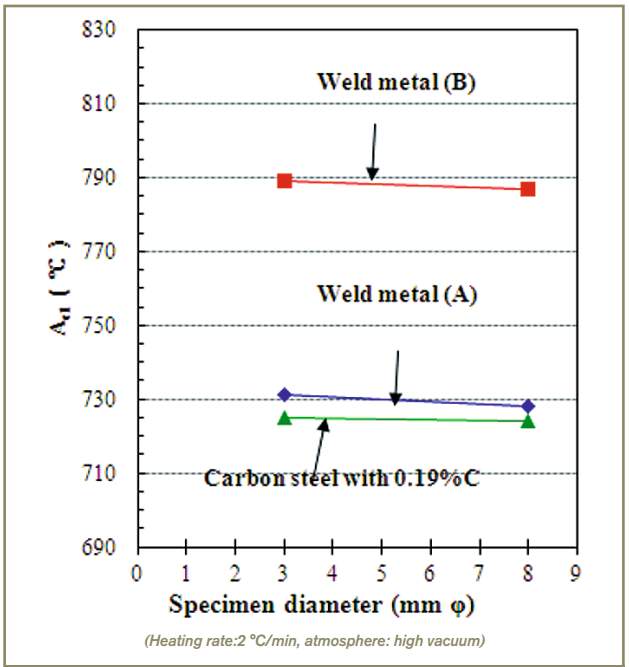

Figure 1 – Effect of specimen size

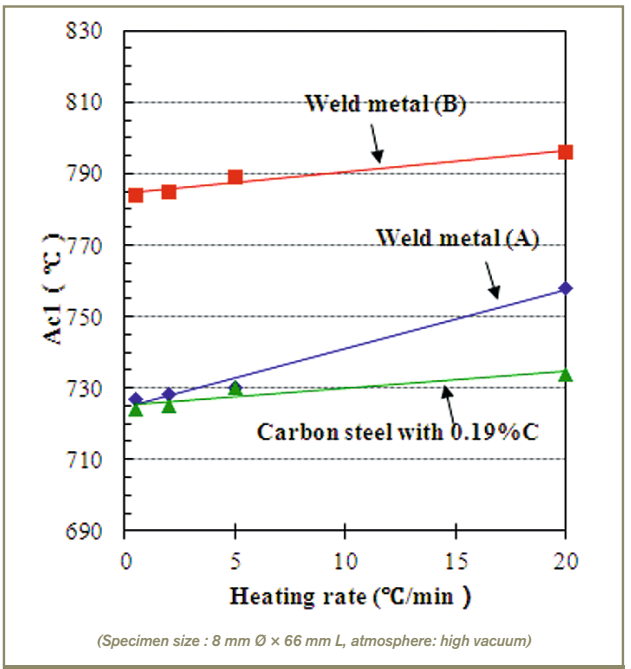

Figure 2 – Effect of heating rate

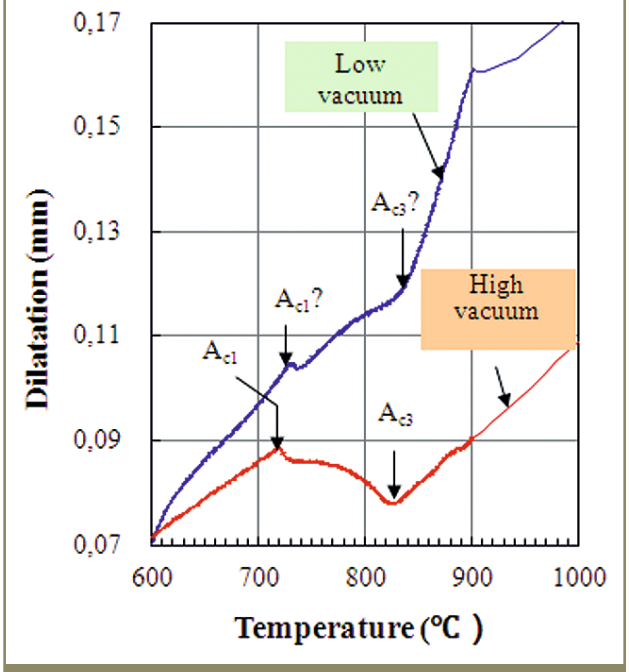

Figure 3 – Dilatation-temperature curves measured in different vacuum degrees

(Specimen: Carbon steel, size:8 mm Ø × 66 mm L, Heating rate:2 ℃/min)

Figure 4 – Views of the specimens after measurement

such high-Cr ferritic heat-resistant steel as Gr. 91. In general, an appropriate PWHT temperature below the A_{C1} of the weld metal is used to provide the weld metal with the temper martensite microstructure that offers better impact toughness and creep-rupture performance. By contrast, the use of a PWHT temperature above A_{C1} is known to cause the weld metal to contain hard fresh martensite and soft ferrite, thereby damaging the weld properties.

To confirm such behaviours, the effects of PWHT temperature on the mechanical properties at room temperature and creep-rupture performance at 600 °C of weld metal (A) with higher Mn+Ni and of weld metal (B) with lower Mn+Ni were investigated. In this study, the A_{C1} of weld metal (A) was determined to be approximately 730 °C and that of weld metal (B), 785 °C according to the measurement results; and the PWHT temperature varied within the range 670-850 °C.

3.1 Effects of PWHT temperature on tensile strength and impact toughness

All-weld-metals were produced in accordance with AWS A5.5 specification [18] by using two kinds of shielded metal arc welding materials to obtain weld metal (A) with high Mn+Ni (2.49 %) and weld metal (B) with low Mn+Ni (1.38 %), and then PWHTs were conducted at 670 °C, 730 °C, 760 °C, 790 °C, 820 °C respectively for weld metal (A), at 720 °C, 760 °C, 800 °C, 850 °C respectively for weld metal (B); PWHT time was four hours for all of the experiments. Room-temperature tension tests and impact tests were conducted in accordance with AWS B4.0 specification [19]. The results of room-temperature tensile strength tests at room temperature are shown in Figure 5, and those of impact toughness, in Figure 6.

Clearly, weld metal (A) with high Mn+Ni and a measured A_{C1} of about 730 °C exhibits the turning point of tendency in both tensile strength and impact toughness vs. PWHT temperature; i.e. when PWHT temperature rises above 760 °C, room-temperature tensile strength starts to increase, and conversely impact toughness starts to decrease. In contrast to this, weld metal (B) with low Mn+Ni and a measured A_{C1} of 785 °C exhibits no turning point of tendency in tensile strength or impact toughness vs. PWHT temperature when PWHT temperature rises, unlike weld metal (A). The clear change in tensile strength and impact toughness of weld metal (A) can be attributed to the formation of a hard, fresh martensite microstructure when PWHT temperature exceeds A_{C1}. And the

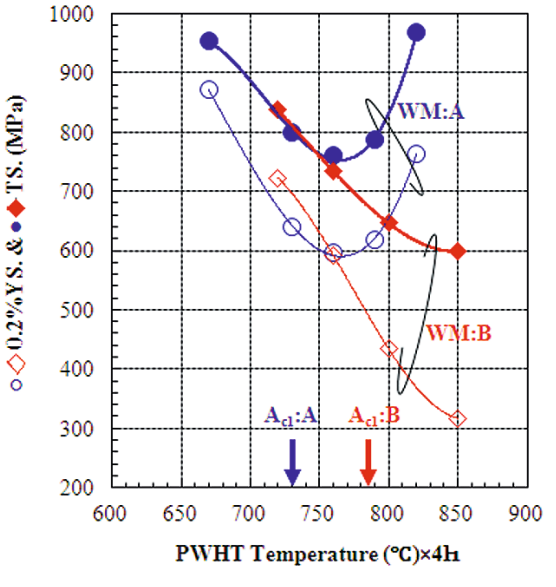

Figure 5 – Tension test results at room temperature

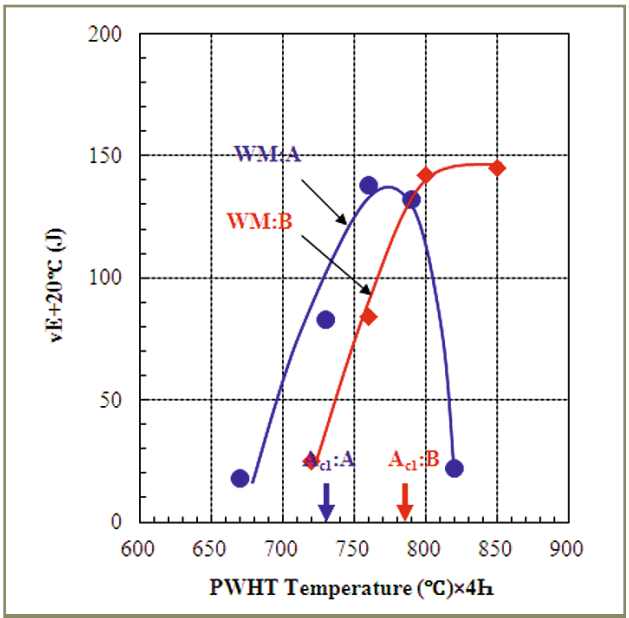

Figure 6 – Charpy impact test results at +20 °C

reason why the PWHT temperature, with which the tendency of tensile strength and impact toughness changed reversely, was about 30 °C higher than A_{C1} can probably be explained by the transformation ratio of fresh martensite. With the dilatation-temperature curve obtained through the measurement of A_{C1}, the reverse transformation at each temperature was calculated relatively and plotted in Figure 7. In the PWHT temperature range that is higher than but close to A_{C1}, the reverse transformation to γ-phase still takes place at a small ratio; hence, even when fresh martensite is formed in the cooling process, its amount should be small and thus insufficient to cause the reverse change in the tendency of tensile strength and impact toughness.

By contrast weld metal (B) exhibits no reverse change in the tendency of tensile strength or impact toughness vs. PWHT temperature unlike weld metal (A), even when PWHT temperature exceeds largely A_{C1} and thus the reverse transformation ratio becomes adequately high. This is presumably because the Mn and Ni contents of weld metal (B) are lower than those of weld metal (A), and hence the PWHT temperature above A_{C1} causes weld metal (B) to form soft ferrite rather than fresh martensite. In order to verify this assumption, the following tests were conducted. Test specimens for measuring A_{C1} were sampled from weld metals (A) and (B) in the as-welded condition. These specimens were heated and held for one hour at a temperature about 30 °C higher than the individual A_{C1}; subsequently, the specimens were cooled at a cooling rate of 2 °C/min (equivalent to the PWHT cooling rate) to develop dilatation-temperature curves (Figure 8) in the cooling process. From the linear expansion trends shown in the figure the microstructures of the specimens can be estimated to a certain degree.

In the case of weld metal (A), the linear expansion taking place at about 400 °C implies martensite transformation or fresh martensite formation. By contrast, the linear expansion taking place in weld metal (B) at approximately 750 °C suggests ferrite formation.

The optical microstructures of the specimens are shown in Figure 9. Obviously, weld metal (A) exhibits no ferrite but weld metal (B) contains ferrite that can be supposed as the white parts. In order to confirm the supposition, both of the microstructures were also observed by Electron Backscattering diffraction (EBSD). Kernel Average Misorientation (KAM) obtained from EBSD pattern can be employed to distinguish between ferrite and martensite through their difference in dislocation density. As KAM is a measure of lattice distortion, it provides average misorientation between the kernel and its close neighbours or the next ones [20], and a KAM map reflects the misorientation between measuring points [21]. From the KAM maps shown in Figure 10, it seems that the dislocation density of white microstructure in weld metal (B) that was observed by optical microscopy is lower than that of the surrounding microstructures. In consideration of the lower dislocation density and dilatation-temperature curves shown in Figure 8, it can be said that ferrite

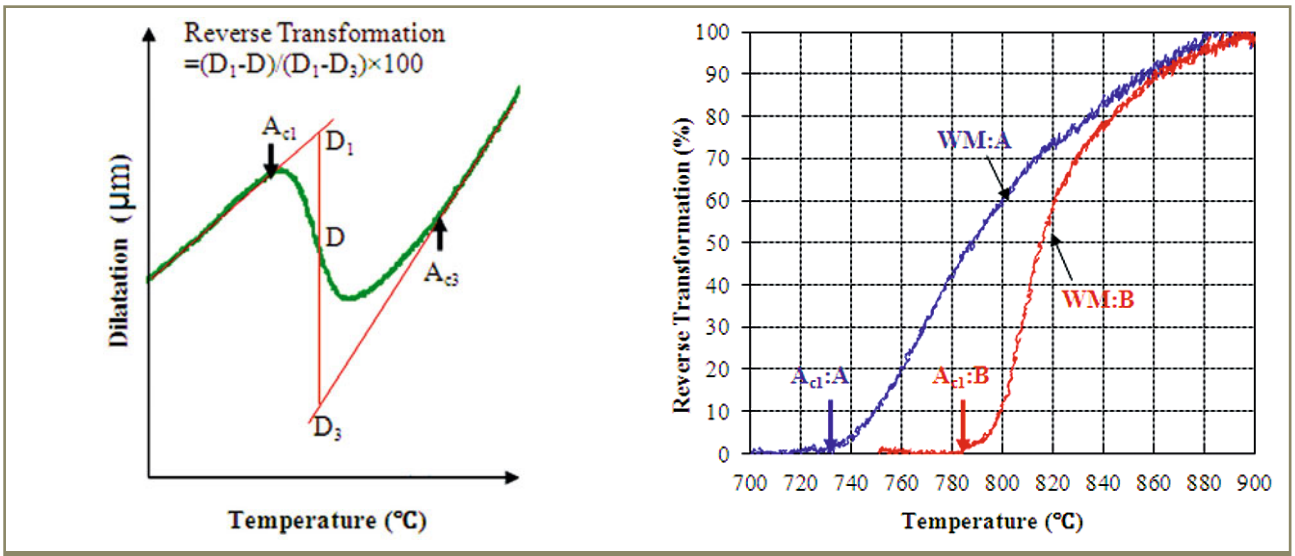

Figure 7 – Reverse transformation at each temperature

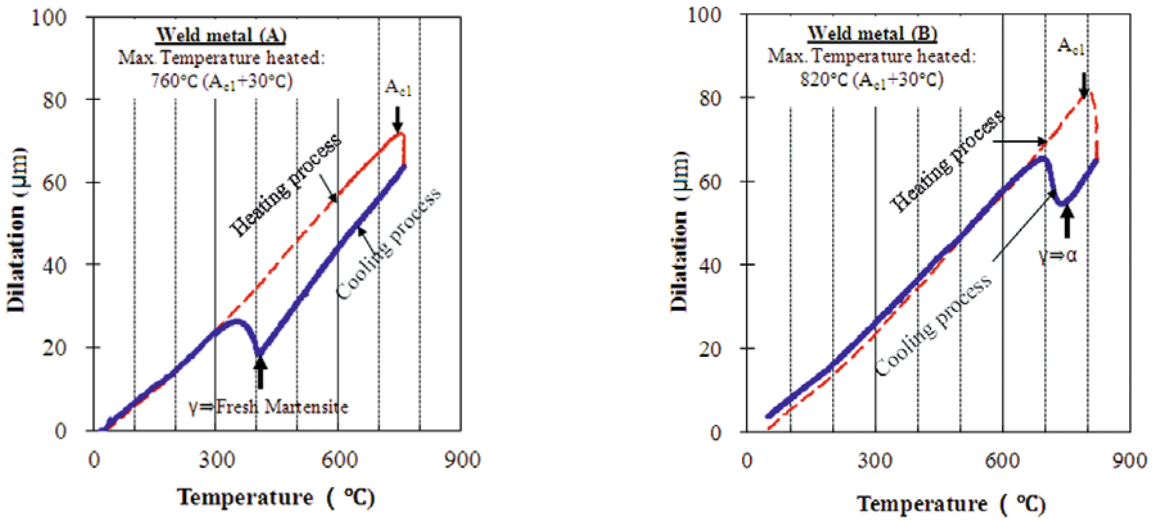

Figure 8 – Dilatation-temperature curves (heating and cooling rate: 2 °C/min)

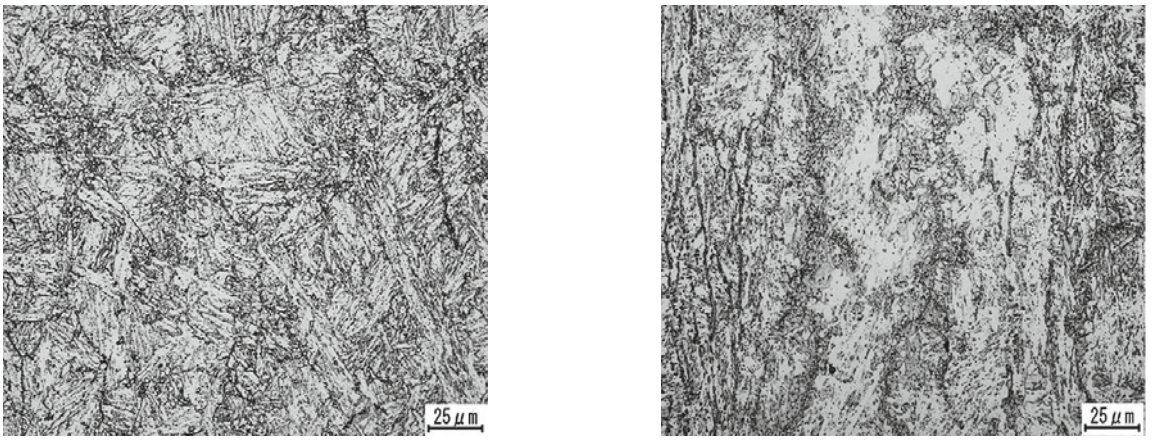

Heated to: 760 °C (A_{c1} + 30 °C)

a) Weld metal (A)

Heated to: 820 °C (A_{c1} + 30 °C)

b) Weld metal (B)

Figure 9 – Microstructures of weld metal (A) and (B)

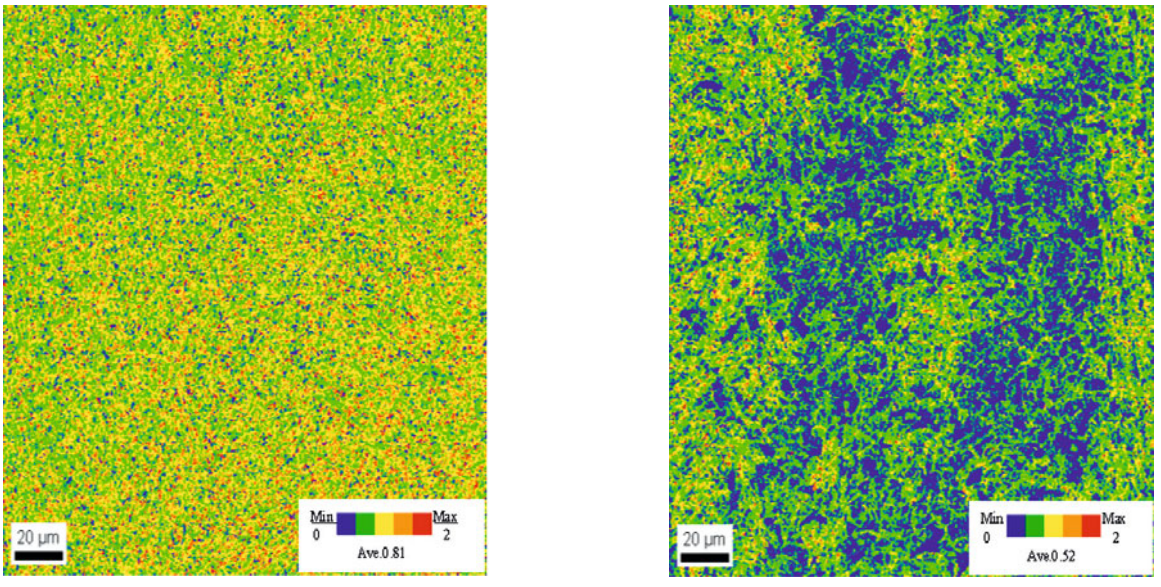

Heated to: 760 °C (A_{c1} + 30 °C)

a) Weld metal (A)

Heated to: 820 °C (A_{c1} + 30 °C)

b) Weld metal (B)

Figure 10 – Kernel average misorientation (KAM) map

was formed in weld metal (B) when PWHT temperature exceeded A_{C1}. That is, it can be assumed that since soft ferrite was formed in weld metal (B), unlike in weld metal (A), no reverse change was observed in the tendency of tensile strength and impact toughness vs. PWHT temperature when PWHT temperature exceeded considerably A_{C1} and thus the reverse transformation ratio became sufficiently high.

3.2 Effects of PWHT temperature on creep-rupture performance

Weld metals (A) and (B) were heat treated at individual PWHT temperatures and were subjected to creep-rupture testing at 600 °C under the two applied stresses of 147 MPa and 108 MPa. Figure 11 shows the relationships between PWHT temperature and the creep time-to-rupture. In the case of weld metal (A) under a high stress of 147 MPa, the creep time-to-rupture turns to increase at the higher PWHT temperature as compared to that in the case of room-temperature tensile strength, but the tendency of transition is similar. By contrast, in the test under a low stress of 108 MPa, the creep time-to-rupture of weld metal (A) decreases continuously as PWHT temperature increases. In the case of weld metal (B), the creep time-to-rupture decreases continuously under both low and high stresses with increasing PWHT temperature.

As mentioned above, weld metal (A) exhibited different tendencies in the creep-rupture performance vs. PWHT temperature between high-stress short-time test and low-stress long-time test. This can presumably be attributed to the difference in the deformation behaviours during creep-rupture test. That is, since an almost uniform microstructural recovery takes place in the entire section of the specimen in the high-stress range [22], the fresh martensite probably increases the dislocation density and solid solution strength, thereby improving the creep-rupture performance. In the low-stress range, since microstructural recovery takes place by priority in the local area near the prior austenite grain boundaries [22] and the solid solution strengthening is reduced by the precipitation of coarse carbides, the fresh martensite did not contribute to the creep-rupture performance. In comparison between weld metals (A) and (B), the creep time-to-rupture of weld metal (B) exhibited a steep descent tendency in the PWHT temperature range above A_{C1}. This was probably because the reversely transformed austenite was transformed to ferrite in the cooling process when weld metal (B) was post-weld heat treated at temperatures above A_{C1}.

4 Examinations of proper PWHT temperature

For weld metals (A) and (B), the proper PWHT temperature was examined by considering the measurements of A_{C1}, the test results of creep-rupture, and observation results of precipitates.

4.1 Proper PWHT temperature vs. A_{C1}

In general, it is said that the PWHT temperature should be lower than A_{C1} of the material to be heat treated. The measurements of A_{C1} of weld metals (A) and (B) were around 730 °C and 785 °C, respectively. Assuming these data to be the true values, the upper limits of the PWHT temperatures of weld metals (A) and (B) should be 730 °C and 785 °C, respectively. However, if 730 °C is specified to be the maximum PWHT temperature for weld metal (A), the weld metal and the heat-affected zone of the base metal cannot be annealed sufficiently and thus adequate weld joint properties including impact toughness may not be obtained. Therefore, the PWHT temperature should

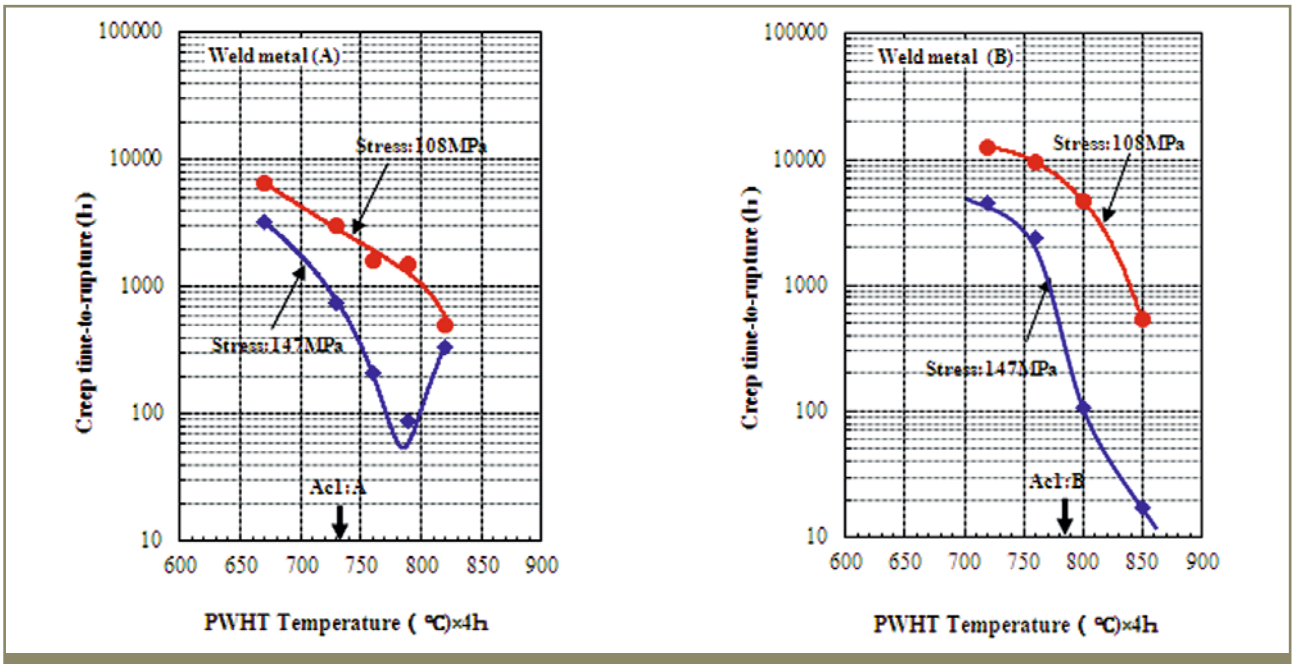

Figure 11 – Relationships between PWHT temperature and the creep time-to-rupture

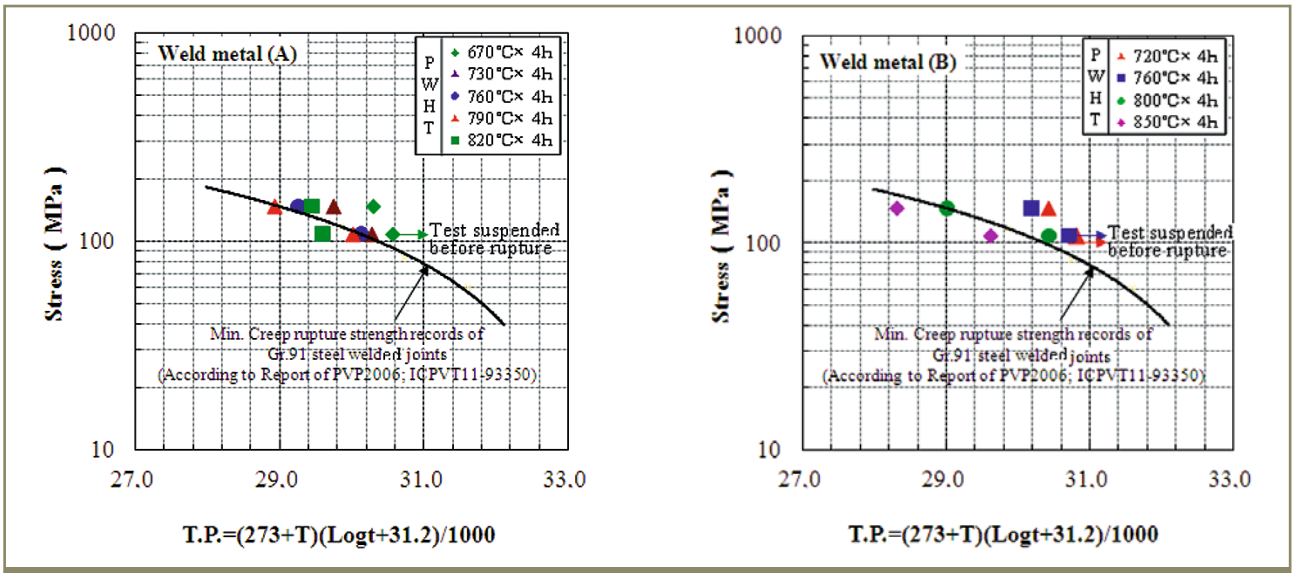

Figure 12 – Creep-rupture master curves

not be determined in a simple manner only from A_{C1} but by taking into account the mechanical properties, such as impact toughness and creep-rupture performance.

4.2 Proper PWHT temperature vs. creep-rupture performance

Gr. 91 steel is used mainly for high-temperature high-pressure equipment such as thermal power boilers, and thus it is exposed to a high-temperature high-pressure environment during operation. Therefore, sufficient creep-rupture performance is required as the most significant quality. Figure 12 shows creep-rupture master curves of weld metals (A) and (B), which includes the creep-rupture strength records of Gr. 91 steel welded joints [23]. From these data, it can be estimated that the maximum PWHT temperatures for weld metals (A) and (B) should be 760 °C and 800 °C respectively, provided that the creep-rupture strength of the weld metal is required to be equal to or higher than that of the welded joints.

4.3 Proper PWHT temperature vs. precipitation behaviours

As regards weld metal (A) in particular, even when PWHT temperature exceeds A_{C1}, no steep descent has been observed in the creep time-to-rupture (Figure 11), and its creep-rupture strength has been proven to be equal to or higher than those recorded for the welded joints (Figure 12). From these facts, it may be no problem to set the maximum PWHT temperature for weld metal (A) to be 760 °C. However, since this temperature is higher than A_{C1}, the authors have further investigated the microstructure of the weld metal to confirm the proper PWHT temperature range. Since the creep-rupture strength of Gr. 91 steel weld metal is enhanced mainly by the carbonitride precipitation, it can be presumed that the amount and profile of the carbonitride precipitates affect significantly the creep-rupture strength. The amount and profile of carbonitride precipitates in the weld metal, which can be a significant information for examining the proper PWHT temperature, are affected markedly by the PWHT conditions as well as the weld metal chemistry and welding conditions.

Figure 13 shows TEM micrographs of weld metal (A) post-weld heat treated at 670 °C, 760 °C, 790 °C, and 820 °C, respectively. These micrographs suggest that there is no difference between 670 °C and 760 °C in the amount and profile of carbonitride precipitates but, in the cases of 790 °C and 820 °C, carbonitride precipitates are likely to be reduced and coarsened.

Furthermore, in order to compare quantitatively the amounts of carbonitride precipitates for individual PWHT temperatures, the extracted residues were analysed. From the analysis results of extracted residues shown in Figure 14, it is obvious that the ingredients of the carbonitride precipitates decrease as PWHT temperature rises above 760 °C. This suggests that the carbonitride dissolution is enhanced by the increase in PWHT temperature, thereby promoting the solid solution of carbonitrides with the matrix. After all, no unusual profile was observed in the precipitates of weld metal (A) post-weld heat treated at temperatures up to 760 °C. From this fact, 760 °C can be deemed to be a reasonable PWHT temperature for weld metal (A), though it exceeds A_{C1} (around 730 °C) of the weld metal.

5 Conclusions

In the present research, two different weld metals for ASME Gr. 91 steel, weld metals (A) and (B) with various Mn+Ni contents, were prepared to measure A_{C1}, and the appropriateness of the measurements was examined. In addition, the effect of PWHT temperature on the mechanical properties of the weld metals was discussed. Following are the summaries of the research.

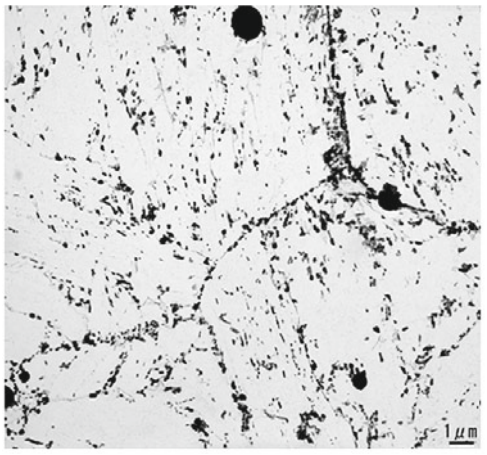

670 °C

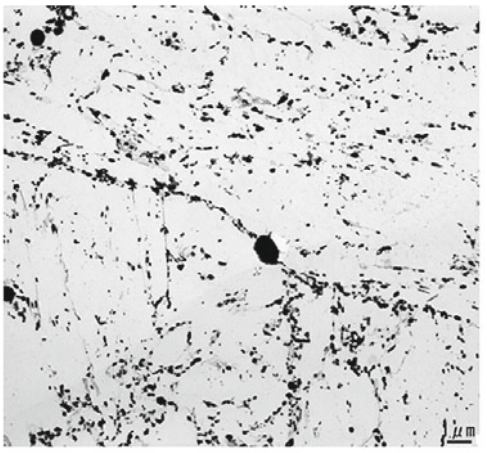

760 °C

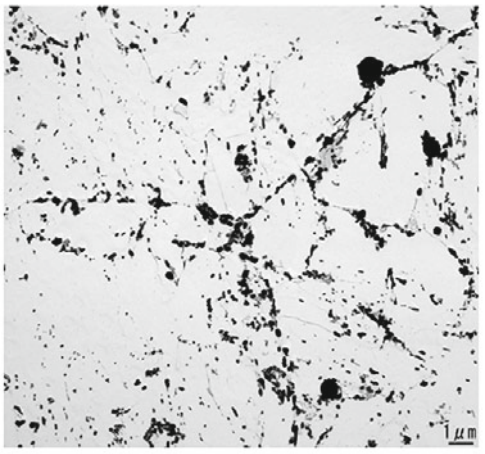

790 °C

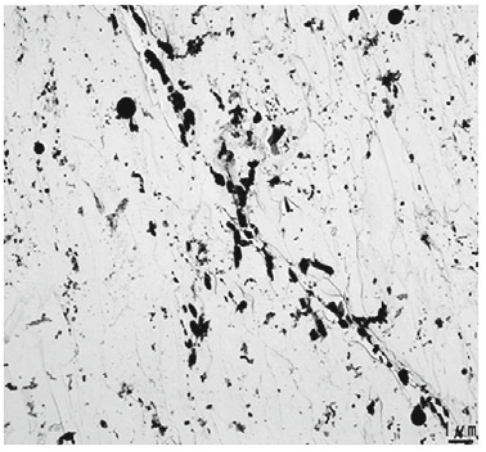

820 °C

Figure 13 – TEM micrographs of weld metal (A) for individual PWHT temperatures

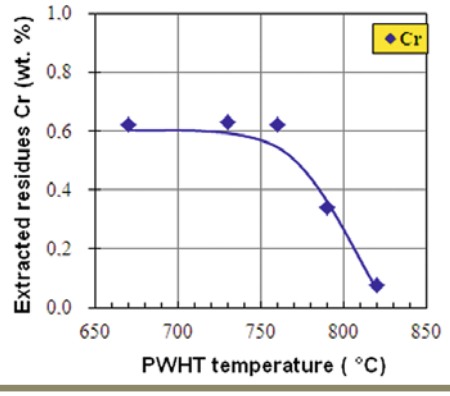

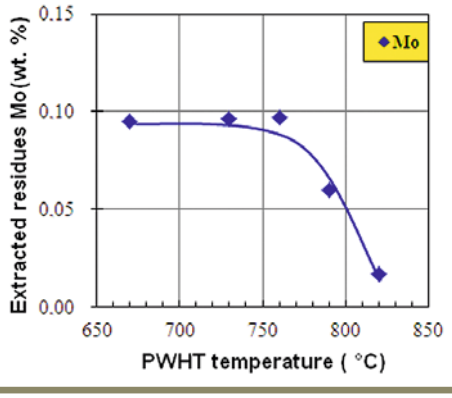

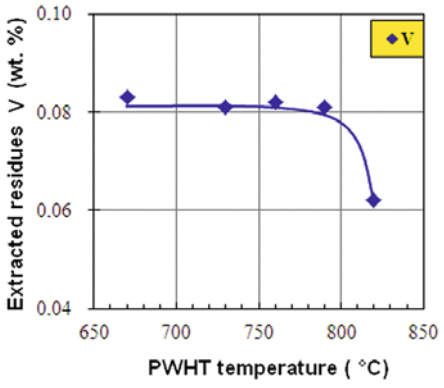

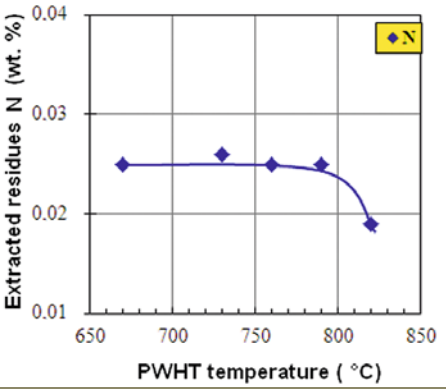

Figure 14 – Analysis results of extracted residues of weld metal (A) for individual PWHT temperature

1. A_{C1} varies according to the measuring method and conditions. From the measurements obtained in this research, the non-contact-type method using a high-accuracy LED in a high-vacuum atmosphere has been deemed most appropriate. As to the measuring conditions, the heating rate should be as slow as possible, and the measuring atmosphere should be controlled so that no oxide film is formed on the specimen surface during measurement.
2. As to the behaviour of the room-temperature mechanical poperties of weld metal (A) vs. PWHT temperature, about 760 °C, not A_{C1} (730 °C) of the weld metal, is the boundary temperature where considerable changes in the tendency can be observed. By contrast, with respect to weld metal (B), no change was observed in the tendency of mechanical properties even when PWHT temperature exceeded A_{C1} of the weld metal. This can presumably be attributed to the lower Mn+Ni content of weld metal (B) as compared to weld metal (A); i.e. the lower Mn+Ni content induced ferrite precipitation when PWHT temperature exceeded A_{C1} of the weld metal.
3. When PWHT temperature exceeds the individual A_{C1}, the creep time-to-rupture of weld metal (B) decreases steeply unlike weld metal (A). This is probably because the reversely transformed austenite is transformed to ferrite during the cooling process when weld metal (B) is heat-treated at a PWHT temperature above A_{C1}.
4. Weld metal (A) exhibits no steep descent in the creep-rupture performance when PWHT temperature is up to 760 °C, showing a performance equal to or higher than the recorded creep-rupture performance of the welded joints. Also, no abnormal microstructure was observed in weld metal (A). These data suggest that 760 °C is the reasonable upper limit for PWHT temperature for weld metal (A), though it exceeds A_{C1} (around 730 °C) of the weld metal. By contrast, in the case of weld metal (B), the creep-rupture performance reduces steeply when PWHT temperature exceeds A_{C1}; hence, the upper limit of PWHT temperature should be lower than A_{C1} (about 785 °C).

References

[1] Sikka V.K.: Development of modified 9Cr-1Mo steel for elevated-temperature service, in Proceedings of Topical Conference on Ferritic Alloys for Use in Nuclear Energy technologies, 1984, pp. 317-327.

[2] Masuyama F.: Metallurgy and heat treatment of heat resistant materials for thermal power, NETSU SHORI, Journal of the Japan Society for Heat Treatment, 2008, vol. 48, no. 4, pp. 237-245.

[3] Ishii R., Tsuda Y., Yamada M. and Kimura K.: Fine precipitates in high chromium heat resisting steels, Tetsu-to-Hagane, The Iron and Steel Institute of Japan, 2002, vol. 88, no. 1, pp. 36-43.

[4] Kimura M., Yamaguti K., Hayakawa M. and Kobayashi K.: Microstructure and grain boundary precipitates in 9-12 % Cr ferritic heat-resisting steels, Tetsu-to-Hagane, The Iron and Steel Institute of Japan, 2004, vol. 90, no. 1, pp. 27-32.

[5] Patric D.S. and Hans V.W.: Controlling heat treatment of welded P91, Welding Journal, June 2006, pp. 42-44.

[6] Newell W.F.: Welding and post weld treatment of P91 steels, Welding Journal, April 2010, pp. 33-36.

[7] Coleman K.K. and Newell W.F.: P91 and beyond, Welding Journal, August 2007, pp. 29-33.

[8] Yamamoto J., Meguro S., Muramatsu Y., Hayakawa N. and Hiraoka K.: Analysis of martensite transformation behavior in welded joint of low transformation- temperature materials, Quarterly Journal of the Japan Welding Society, 2007, vol. 25, no. 4, pp. 560-568.

[9] Babu S.S., David S.A., Santella M.L., Vitek J.M., Specht E.D. and Elmer J.W.: Modeling and characterization of non-equilibrium weld microstructure evolution, 7th International Seminar Numerical analysis of Weldability, Seggau Graz Austria, 2003.

[10] Santella M. and Shingledecker J.: Advanced pressure boundary materials, Oak Ridge National Laboratory, Oak Ridge, Tenessee, USA.

[11] Tokunaga S. and Masuyama F.: Phase transformation behavior of Gr. 91 ferritic steel around the A_{C1} temperature, CAMP-ISIJ, 2008, vol. 21, p. 1066.

[12] Alexandrov B.T. and Lippold J.C.: Single sensor differential thermal analysis of phase transformations and structural changes during welding and post weld heat treatment, Doc. IIW-1843, Welding in the World, 2007, vol. 51, no. 11/12, pp. 48-59.

[13] Kumar A., Choudhary B.K., Laha K., Jayakumar T., Bhanu Sankara Rao K. and Raj B.: Characterisation of microstructure in 9 % chromium ferritic steels using ultrasonic measurements, Transactions of the Indian Institute of Metals, October 2003, vol. 56, no. 5, pp. 483-497.

[14] ASTM 1033-4, Standard practice for quantitative measurement and reporting of hypoeutictoid carbon and low-alloy steel phase transformations.

[15] SEP 1681: Guidelines for preparation, execution and evaluation of dilatometric transformation tests on iron alloys.

[16] Raju S., Ganesh B.J., Banerjee A. and Mohandas E.: Characterization of thermal stability and phase transformation energetics in tempered 9Cr-1Mo steel using drop and differential scanning calorimetry, Materials Science and Engineering A, 2007, vol. 465, no. 1-2, pp. 29-37.

[17] Santella M.L., Swindeman R.W., Reed R.W. and Tanzosh J.M.: Martensite formation in 9 Cr-1 Mo steel weld metal and its effect on creep behavior Oak Ridge National Laboratory, Oak Ridge, Tenessee, USA.

[18] AWS A5.5:2006: Specification for low-alloy steel electrodes for shielded metal arc welding.

[19] AWS B4.0:2007: Standard Methods for Mechanical Testing of Welds.

[20] Man O., Pantělejev L. and Pešina Z.: EBSD analysis of phase compositions of trip steel on various strain levels, Materials Engineering, 2009, vol. 16, no. 2, pp. 15-21.

[21] Ohtani T., Yin F.X. and Kamada Y.: Microstructure and non-destructive evaluation of creep damage in martensite stainless steel, Journal of the Society of Material Science, Japan, 2009, vol. 58, no. 2, pp. 136-142.

[22] Hideaki K., Kimura K. and Abe F.: Degradation of Mod. 9Cr-1Mo Steel during long-term creep deformation, Tetsu-to-Hagane, The Iron and Steel Institute of Japan, 1999, vol. 85, no. 11, pp. 841-847.

[23] Tabuchi M. and Takahashi Y.: Evaluation of creep strength reduction factors for welded joints of modified 9Cr-1Mo steel (P91), ASME Conference Proceedings, ASME 2006 Pressure Vessels and Piping, ICPVT11 Conference, PVP2006-ICPVT11-P93350, July 23-27, 2006, pp. 529-534.

About the authors

Mr. Liang CHEN (chin.ryo@kobelco.com), and Mr. Ken YAMASHITA (yamashita.ken@kobelco.com), are both with Kobe Steel Ltd., Welding Business, Technical Development Dept., Fujisawa (Japan).